Scientific Reports Title to see here (20 words or less)

Rachel LeCover[1] **and Jeffrey D. Varner**[1,*]

[1]Affiliation, School of Chemical and Biomolecular Engineering, Ithaca NY, 14852, USA
[*]jdv27@cornell.edu

ABSTRACT

Example Abstract. Abstract must be under 200 words and not include subheadings or citations. Example Abstract. Abstract must be under 200 words and not include subheadings or citations. Example Abstract. Abstract must be under 200 words and not include subheadings or citations. Example Abstract. Abstract must be under 200 words and not include subheadings or citations. Example Abstract. Abstract must be under 200 words and not include subheadings or citations. Example Abstract. Abstract must be under 200 words and not include subheadings or citations. Example Abstract. Abstract must be under 200 words and not include subheadings or citations.

Please note: Abbreviations should be introduced at the first mention in the main text – no abbreviations lists. Suggested structure of main text (not enforced) is provided below.

Introduction

The rate at which a heart beats is determined, in part, by the sympathetic and parasympathetic portions of the nervous system. When the sympathetic nervous system is stimulated, it releases epinephrine and norepinephrine. Norepinephrine increases heart rate by increasing the rate of depolarization in pacemaker cells and increases contractability through the phosphorlation of several types of receptors.[1] The parasympathetic system releases acetylcholine which decreases heart rate and contractibility through its binding to M_2 receptors. These two systems, often described as an accelerator and a brake, are not totally independent on each other, rather, they interact through second messengers cAMP and cGMP.[2] Heart rate is also controlled by the baroreflex system. The baroreflex system consists of baroreceptors, tension sensitive nerve endings found in the circulatory system.[3] When they sense a change in pressure, they cause a change in the frequency of nerve activity. When pressure (and stretch) rapidly increase, so does the baroreceptor firing rate.[4] This effects of this signal are not instantaneous, rather, there is a time delay on the order of seconds before the sympathetic and parasympathetic nervous systems respond.[3]

This control process leads to a negative feedback loop, where if the mean arterial pressure increases, vasodilation and bradycardia occur, whereas if the mean arterial pressure decreases, the opposite, vasoconstriction and tachycardia occur.[1] In patients suffering from hypertension, the controlers in this loop get reset to the higher pressure, but the set point can be changed again where blood pressure returns to normal levels.[5]

Olufsen and Ottesen have developed models of heart rate based on blood pressure measurements.[6] From the blood pressure measurement, the model predicts a firing rate for different types of receptors, which is then used to predict the response times of the parasympathetic and sympathetic nervous system. The response times are then used to predict dimensionless norepinephrine and acetylcholine concentrations, which are finally used to predict heart rate.

We used the MIMIC II Waveform Database as the source of the pressure and heart rate data used to test this model.[7] MIMIC contains de-identified data from patients who visited the Beth Israel Deaconess Medical Center ICU. This database contains a wealth of information: diagnoses, demographics, clinical data, such as heart rate and intravenous medications as well as laboratory results. A subset of the MIMIC II Waveform Database has been linked to patients found in the MIMIC II Database, allowing us to combine the waveforms with demographic information. From this subset, we selected patients that had numerics records with data recorded once per second with more than five data points available in the first 10 minutes of recorded data, giving us 273 patients meeting this criteria. To our knowledge, this is the first study to attempt to model heart rate as a function of blood pressure for such a large number of patients. Additionally, many previous studies were performed with healthy patients, in contrast, this study focuses on intensive care unit patients.

Model Formulation

The model assumes changes in arterial wall stretch are proportionate to filtered blood pressure, $\dot{\bar{p}} = \alpha(-\bar{p}+p)$ where α is a gain, $\bar{p}$ is the filtered blood pressure, and p is the patient's measured blood pressure. From $\bar{p}$, we can predict the nervous

system firing rate, $n = \sum_i n_i + N,\ i = 1,2$ where N is a baseline firing rate and n_i corresponds to the firing rate of nerve fibers of type i. The firing rates for nerves of type i are computed as:

$$\frac{dn_i}{dt} = \kappa_i \frac{d\bar{p}}{dt} \frac{n(M-n)}{(M/2)^2} - \frac{n_i}{\tau_i}, i = 1,2 \tag{1}$$

where M is the maximum firing rate, and τ_i is the time scale for nerves of type i. The firing rate information is compiled by the central nervous system, which then determines the the sympathetic and parasympathetic outputs, f_{sym} and f_{par}, respectively. The parasympathetic output is given by $f_{par} = n/M$, while sympathetic output takes the form:

$$f_{sym} = \frac{1 - n(t-\tau_d)/M}{1 + \beta f_{par}} \tag{2}$$

With these outputs, we can determine the dimensionless concentrations of acetylcholine, c_{ach} and noradrenaline, c_{nor}:

$$\frac{dc_j}{dt} = \frac{f_i - c_j}{\tau_j} \tag{3}$$

where each τ_j represents a time scale. Finally, the heart rate is calculated from h_0, the intrinsic heart rate, and m_{nor} and m_{ach}, which are weights for the contributions of acetylcholine and norepinephrine to heart rate $h = h_0(1 + m_{nor}c_{nor} - m_{ach}c_{ach})$.

Results

One Dimensional Optimization of Parameters

We minimized averaged the mean squared error per patient using the Nelder Mead algorithm as implemented in Julia package NLopt. We forced all of the parameters to be non-negative as to be biologically correct.The original and estimated values of the parameters are shown in Table 1.

Within the estimated parameter set, the value of N, the baseline firing rate increased, and both k_1 and τ_1, representing a change in the response rate of the faster firing baroreceptors in the model. Baroreceptors are generally divided into three groups, depending on their transmission speeds (on the order of half a second, five seonds, and five hundred seconds), but this model only includes two types.[?] The increase in τ_1 and the decrease in τ_2 in the estimated parameter set may be the result of oversimplification.

The baseline heart rate (h_0) decreased slightly, to 88 bpm, from the initial 100 bpm. Both τ_{ach} and m_{ach}, which determine how acetylcholine plays into the model, decreased dramatically in the estimated parameter set, with the reduction in m_{ach} reducing the effects of a change in acetylcholine on heart rate, and the decrease in τ_{ach} increasing the rate of acetylcholine change. The estimated parameter set reduced the averaged mean squared error to 352 from 1167. As seen in Figure 1, the estimated parameters slightly overestimate heart rate for this patient, but they perform far better than the original parameters, which severely underestimate the heart rate. This behavior is typical of the model on patients in this study.

k_2 and β were held constant as to reduce the search space, as done by Olufsen and Ottesen. Additionally, when they were allowed to vary during the optimization, the parameter set generated had very small values for m_{ach} and m_{nor}, resulting in a predicted heart rate that was basically constant at h_0. While this set of the parameters did mimimize the MSE, it did not capture the intrinsic varation in heart rate. α, the parameter used to smooth the pressure data was held constant at 1.5 to smooth the data with a minimal phase shift. The maximum firing rate, M, was held constant, as it only appears in this system of equations by normalizing n. The sympathetic nervous system delay, τ_d, was held constant, owing to the propagation of discontinuities.[8]

Clustering

We clustered the patients based on their age, average heart rate, and SAPS (Simplified Acute Physiology) score, a measure that estimates a patient's risk of death within an intensive care unit.[9] We used the patient's average SAPS since some patients had multiple admissions resulting in more than one blood pressure-heart rate track. Through the use of the Clustering Julia package, we created up to 26 clusters based on these variables, and scored each cluster with the sum of its silhouettes, where a higher score means that each member of the cluster is more similar to the other members of the clusters.[10] We found that grouping the patients into two clusters gave the highest score and therefore the best clustering. The sum of silhouettes as a function of number of clusters is shown in 5, and the patients by cluster in 2. Cluster 1 patients (n = 165), shown in white, tend to have a lower average heart rate (73 BPM compared to 88 BPM), and be older than patients in cluster 2 (n = 108) (69 years vs 59 years, on average).

Multidimensional Optimization

We used the Julia language POETs package, which combines simulated anealing with Pareto optimality to generate families of best parameters.[11] Using the two clusters formed by k-means, we minimized the averaged mean squared error to create these parameter families. We utilized a monotonically decreasing cooling schedule with five iterations at each temperature. The trade off curve generated using α = .9 is shown in 8, and with α =.5 in 9. We used the parameter families from the slower cooling for further analysis. To decrease the time necessary to perform the simulated annealing, we utilized Julia's transparent parallelization capabilities. With the @parallel (+) operator, we were able to calculate patient's mean squarred errors in parallel. The speed up from parallelization is shown in 6. We then selected the ten best sets of parameters from each cluster to examine the performance of the model with the new parameters. A sample patient from cluster 1 is shown in 3, and from cluster 2 in 4. The new parameter families reduced the averaged mean squared error even further than the parameters estimated using Nelder Mead-the ten best families for cluster 1 reduced the averaged mean squared error to 135 or less, and for cluster two, the averaged mean squared error was reduced to 178, or less.

Both of the families had fairly similar values for m_{nor} and m_{ach}, however, cluster 1 had a larger value of N, the resting firing rate than cluster 2. Cluster 1 contains the older patients, on average, suggesting that the resting firing rate may be age dependent. The differences in average heart rate between the clusters apparent in the clustering are appearent in the difference in h_0 between the two clusters, with cluster 2 having a faster base line heart rate, at $1.749 \pm .05$ beats per second, corresponding to 104.95 ± 3 beats per minute, compared to 74.4 ± 4 beats per minute for cluster 1.

Sensitivity Using Finite Differences

The derivatives of all parameters were estimated using central differences.

$$\frac{dh}{d\theta_j} = \frac{h(\theta_0 + \frac{e_j}{2}) - h(\theta_0 - \frac{e_j}{2})}{\delta} \tag{4}$$

where $\delta = 10^{-8} * \theta_j$ and e_j is a vector of length δ in the j^{th} direction. To collapse the time dimension, we calculated overall state sensitivity coefficients.[12]

$$S_{0j}(t) = \frac{1}{n_s} p_j \left(\sum_{k=1}^{n_t} \sum_{i=1}^{n_s} \left[\frac{1}{x_i} \frac{dx_i(t_k)}{dp_j} \right]^2 \right)^{1/2} \tag{5}$$

where n_s = 1, as h is the only state variable and n_t is the number of time points available for that patient. We calculated sensitivites of parameters that were optimized and not that of those held constant.

Single Objective Sensitivity

From the original values provided by Olufsen and Ottesen, we found that h_0 was the most sensitive parameter, followed by N, m_{ach}, and m_{nor} in that order, of the parameters estimated. Of the four most sensitive equations, three of them (h_0, m_{ach} and m_{nor}) appear directly in the equation for heart rate, and N indirectly appears, as both c_{ach} and c_{nor} are functions of N. The four estimated parameters that were the most sensitive in our study were among the five most sensitive parameters found by Olufsen and Ottesen, as seen in 3. However, k_2 showed a very high degree of sensitivity in both the original and estimated parameter set, even more so than any of the estimated parameters. It also had the highest varriance in sensitivity, due to the fact that some patients exhibited a sensitivity to k_2 that was an order of magnitude larger than the mean.

Between the estimated and the original parameters, the sensitivity of h_0 barely changed, but N became much less sensitive in the estimated parameter set and m_{ach} increased in sensitivity. This appearent change in sensitivity originates from the method of calculation, where the sum is divided by the value of the parameter. As N increased in the estimated parameter set, dividing by this new value decreased the overal state sensitivity coefficent, while the opposite is true for m_{ach}.

Multiobjective Sensitivity

For the multiobjective case, we used the same finite differences, but averaged them not only over the patients, but over the families of parameters-the ten best for each cluster. As with the single objective case, h_0 is the most sensitive parameter, followed by N, as seen in 7 for both clusters, but N is about two times as sensitive in cluster 2 as in cluster one, whereass h_0 has nearly the same sensitivity for both clusters. If one were to rank the parameters by sensitivity, the ordering of the four most sensitive parameters between the two clusters is idenitical, however, τ_{nor} in cluster 2 is approximately an order of magnitude less sensitive than in cluster 1 and τ_{ach} is nearly three orders of magnitude less senstivie in cluster 2 compared to cluster 1. Of the parameters held constant during optimization, k_2 showed the highest degree of sensitivity in both clusters, which corresponds to the sensitivity found in the single objective case.

If we were to compare to the parameters estimated by Nelder Mead, we find similar sensitivites in h_0 and N as well as in m_{ach} and m_{nor}. The sensitivities in all of the τs included in the model is much smaller in the multiobjective case than in the

single objective case. Part of this difference in sensitivity may arise from the differences in value found for these parameters by the different methods of optimization.

Discussion

We estimated three sets of parameters that can be used to predict heart rates of patients in intensive care units. The accuracy of the model was much improved when patients were grouped by their characterstics. This improvement in accuracy is likely mostly based on that the resting heart rate of the patients in clusters more accurately matched h_0, the resting heart rate in the model, since h_0 was shown to be the most sensitive parameter in the model.

We discovered that one of the parameters found to be fairly unsensitive in previous work, k_2, was surprisingly sensitive in this work. It was held constant during optimization as previous work pointed to it being a very unsensitive parameter, but it proved to be very sensitive in all cases. Future work may involve estimating a better value for the gain on this type of barroreceptor.

The model used has several shortcomings. This model oversimplifies the process of heart rate regulation. It does not include cardiac sypathetic afferrent reflex, which is sensitive to both mechanical and chemical inputs.[13] It can only be used for short time scales, as it does not include the slower acting renin-agiotensin-aldostrone system, which determines blood volume, and therefore blood pressure.[1] The model only considers two vassoctive agents when there are many more and does not attempt to capture the effects of respiration rate. Nevertheless, it does captures the dynamics of the system at short time scales.

Methods

All calculations were carried out Ubunutu 16.04 using Julia version .0.4.5, with 7.7 GB of available RAM on a Intel Core i7-6700 CPU @ 3.40GHz. Differential equations were solved using the ODE package, with solvers ode23 and ode78, with an absolute and relative tolerance of 10^{-8}. Single objective optimization was perfomed using the Nelder Mead algorithm, as implimented in the Julia package NLopt, and multiobjective optimization was performed using the POETs package.

Since pressure data was given in a discrete format, we linearly interpolated between values when neccessary, as pressure is an input to the system of differential equations. We used the pressure data recorded at 1 Hz as well as the heart rate data at 1 Hz from the MIMIC II Waveform Database, numerics section. We extracted data from the database using rdsamp and stored it locally as text files that were then read into the model.

References

1. Boron, W. F. & Boulpaep, E. L. *Medical physiology* (Elsevier Health Sciences, 2016).
2. Olshansky, B., Sabbah, H. N., Hauptman, P. J. & Colucci, W. S. Parasympathetic nervous system and heart failure pathophysiology and potential implications for therapy. *Circulation* **118**, 863–871 (2008).
3. Ottesen, J. T. Modelling of the baroreflex-feedback mechanism with time-delay. *Journal of mathematical biology* **36**, 41–63 (1997).
4. NEGATIVE, A. B. A. A. Reflexes that control cardiovascular function (1999).
5. Oparil, S., Zaman, M. A. & Calhoun, D. A. Pathogenesis of hypertension. *Annals of internal medicine* **139**, 761–776 (2003).
6. Olufsen, M. S. & Ottesen, J. T. A practical approach to parameter estimation applied to model predicting heart rate regulation. *Journal of mathematical biology* **67**, 39–68 (2013).
7. Saeed, M. *et al.* Multiparameter intelligent monitoring in intensive care ii (mimic-ii): a public-access intensive care unit database. *Critical care medicine* **39**, 952 (2011).
8. Baker, C. T. & Paul, C. A. Pitfalls in parameter estimation for delay differential equations. *SIAM Journal on Scientific Computing* **18**, 305–314 (1997).
9. Le Gall, J.-R., Lemeshow, S. & Saulnier, F. A new simplified acute physiology score (saps ii) based on a european/north american multicenter study. *Jama* **270**, 2957–2963 (1993).
10. Rousseeuw, P. J. Silhouettes: a graphical aid to the interpretation and validation of cluster analysis. *Journal of computational and applied mathematics* **20**, 53–65 (1987).
11. Bassen, D., Vilkhovoy, M., Minot, M., Butcher, J. T. & Varner, J. D. Jupoets: A constrained multiobjective optimization approach to estimate biochemical model ensembles in the julia programming language. *bioRxiv* 056044 (2016).

12. Stelling, J., Gilles, E. D. & Doyle, F. J. Robustness properties of circadian clock architectures. *Proceedings of the National Academy of Sciences of the United States of America* **101**, 13210–13215 (2004).

13. Du, Y.-H. & Chen, A. F. A "love triangle" elicited by electrochemistry: complex interactions among cardiac sympathetic afferent, chemo-, and baroreflexes. *Journal of Applied Physiology* **102**, 9–10 (2007).

Acknowledgements (not compulsory)

Acknowledgements should be brief, and should not include thanks to anonymous referees and editors, or effusive comments. Grant or contribution numbers may be acknowledged.

Author contributions statement

Must include all authors, identified by initials, for example: A.A. conceived the experiment(s), A.A. and B.A. conducted the experiment(s), C.A. and D.A. analysed the results. All authors reviewed the manuscript.

Additional information

To include, in this order: **Accession codes** (where applicable); **Competing financial interests** (mandatory statement). The corresponding author is responsible for submitting a competing financial interests statement on behalf of all authors of the paper. This statement must be included in the submitted article file.

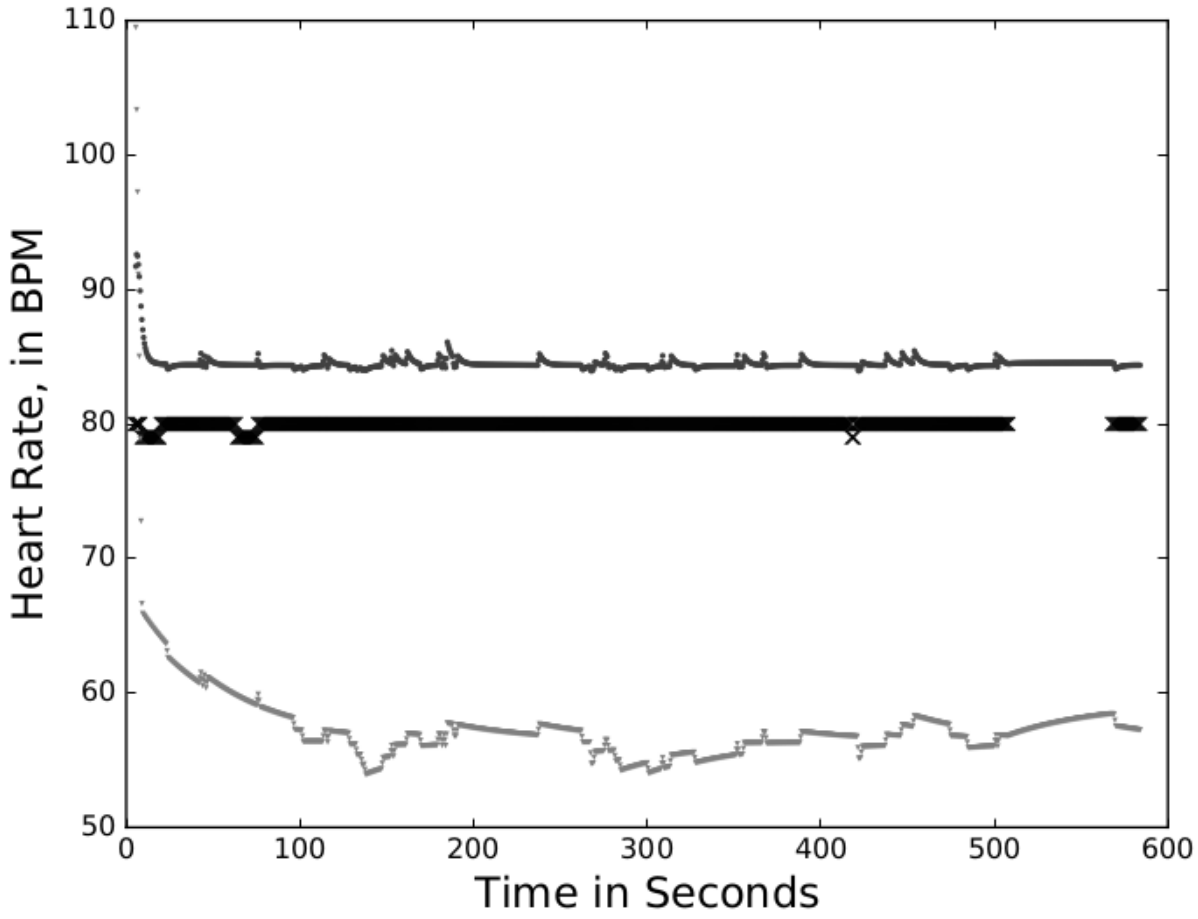

Figure 1. The black xs are the measured heart rate, the dark gray is the model prediction using the original parameters and the light gray is the model prediction using the original parameters.

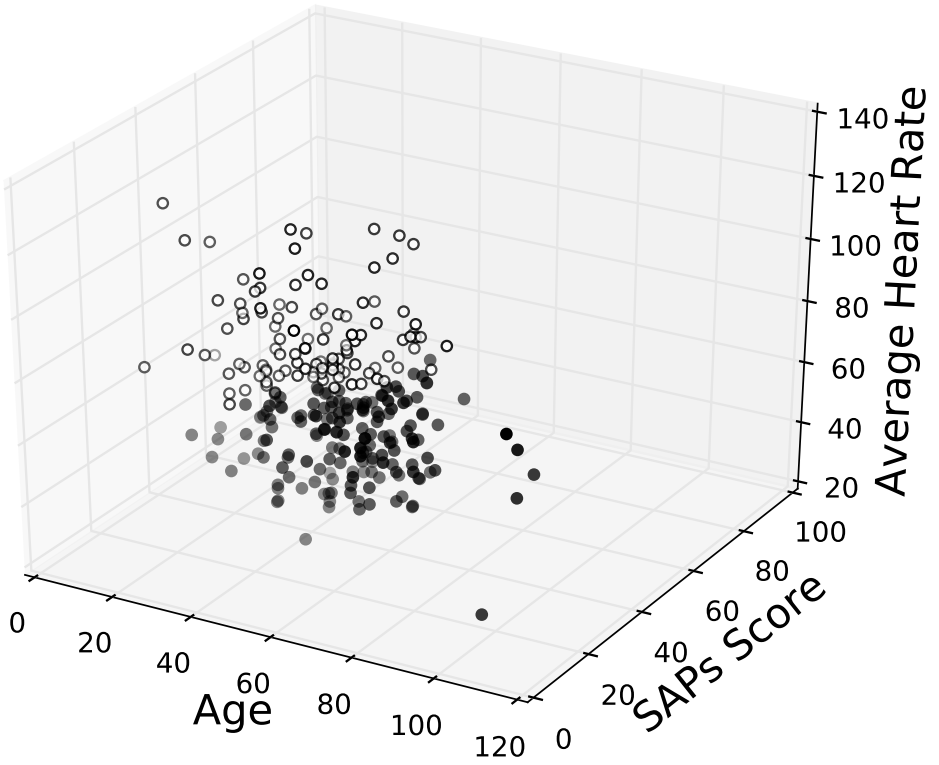

Figure 2. The patients, clustered into two groups.

Table 1. Original and estimated parameter values. The bolded parameters were held constant.

Parameter	α	N	M	k_1	k_2	τ_1	τ_2	τ_{ach}	τ_{nor}	β	h_0	m_{nor}	m_{ach}	τ_d
Original Value	**1.5**	75	**120**	1.5	**0.5**	0.5	250	0.5	0.5	**6**	1.67	0.96	0.7	**7**
Parameter Estimations from MIMIC II Data	**1.5**	107.33	**120**	41.139	**0.5**	14.062	202.925	2.94E-05	8.156	**6**	1.474	0.165	5.20E-02	**7**

Table 2. Average parameter values for the 10 best sets per cluster. Data is reported as mean $\pm$ stdev. Bolded columns were held constant.

Cluster	α	N	M	k_1	k_2	τ_1	τ_2	τ_{ach}	τ_{nor}	β	h_0	m_{nor}	m_{ach}	τ_d
1	**1.5**	50.36 ± 9	**120**	$.9566 \pm .3$	**0.5**	$.1854 \pm .13$	127.31 ± 46	$.5968 \pm .4$	$.3176 \pm .06$	**6**	$1.245 \pm .006$	$.1816 \pm .02$	$.0434 \pm .004$	**7**
2	**1.5**	37.98 ± 9	**120**	$1.379 \pm .7$	**0.5**	$.3621 \pm .11$	82.88 ± 33	$.1410 \pm .06$	$.1688 \pm .04$	**6**	$1.749 \pm .05$	$.1609 \pm .02$	$.0962 \pm .06$	**7**

Table 3. Average Overall State Sensitivity Coefficents For Single Objective Case

Parameter set	S_α	S_N	S_M	S_{k_1}	S_{k_2}	S_{τ_1}	S_{τ_2}	$S_{\tau_{ach}}$	$S_{\tau_{nor}}$	S_β	S_{h_0}	$S_{m_{ach}}$	$S_{m_{nor}}$	S_{τ_d}
original parameters	3.99 ± 2	15.26 ± 4	$.0069 \pm .002$	$.0792 \pm .04$	142.61 ± 30	$.0739 \pm .04$	$.0156 \pm .004$	$.0540 \pm .013$	$0.00055 \pm 4E-4$	$.113 \pm .13$	19.9 ± 6	$.574 \pm .7$	14.6 ± 4	$.085 \pm .09$
estimated parameters	78 ± 250	2.24 ± 5	$.329 \pm .6$	$.89 \pm 3$	86 ± 400	1.20 ± 4	$.61 \pm 3$	0.52 ± 2	4.34 ± 1.9	$.52 \pm 5$	20.1 ± 6	6.79 ± 2	$.83 \pm 1.9$	$4.13E-7 \pm 3E-6$

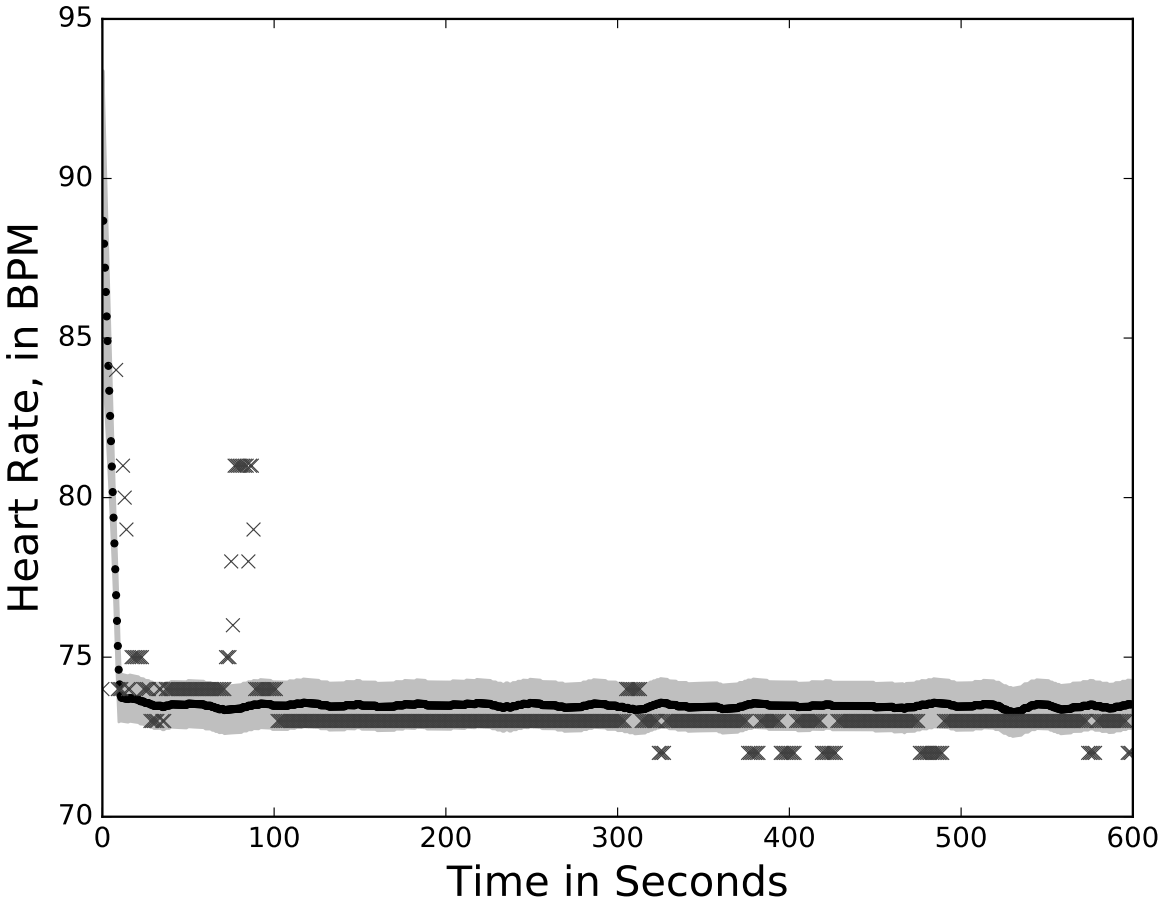

Figure 3. Performance of the model on a patient in cluster 1. The x represent the true heart rate, the black dots are the mean model prediction from the family of best parameter sets, and the grey gives a 95% confidence interval.

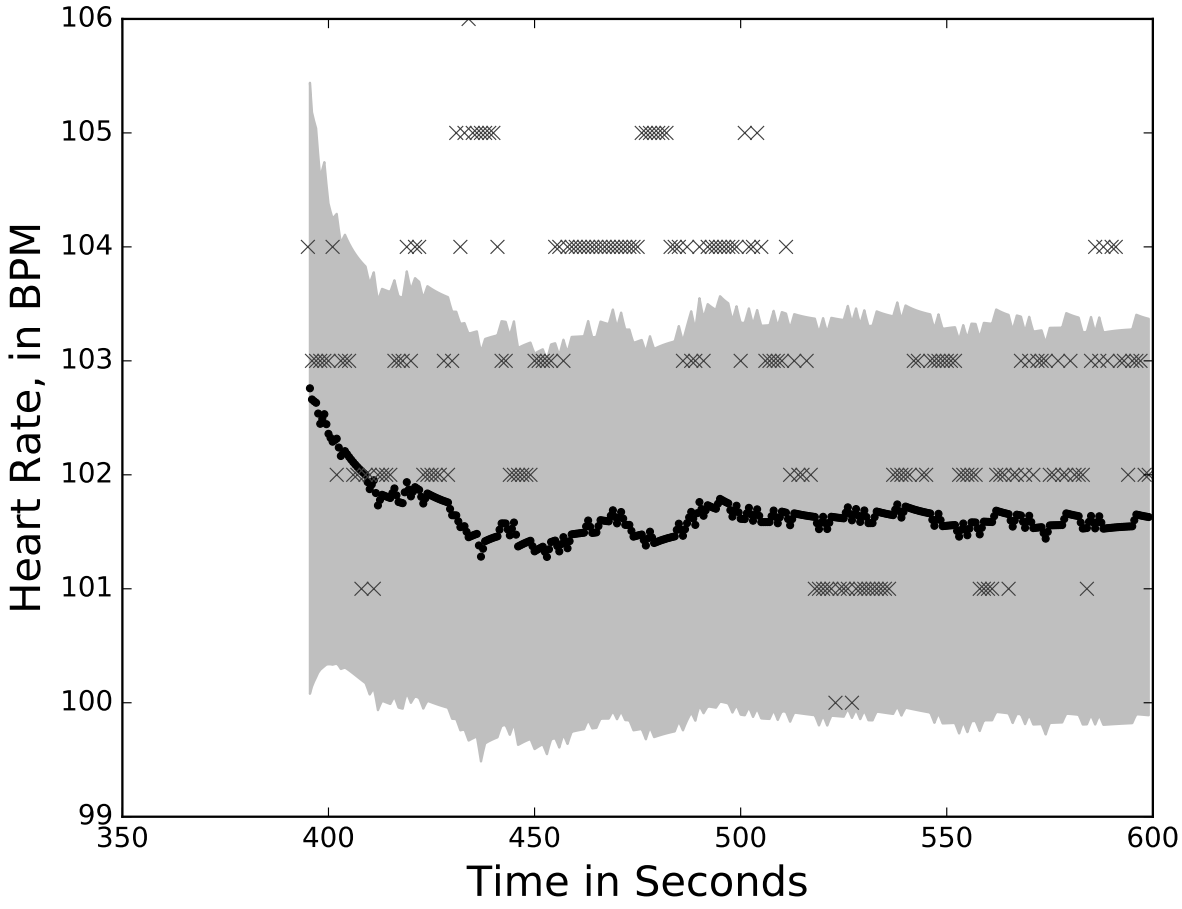

Figure 4. Performance of the model on a patient in cluster 2. The x represent the true heart rate, the black dots are the mean model prediction from the family of best parameter sets, and the grey gives a 95% confidence interval.

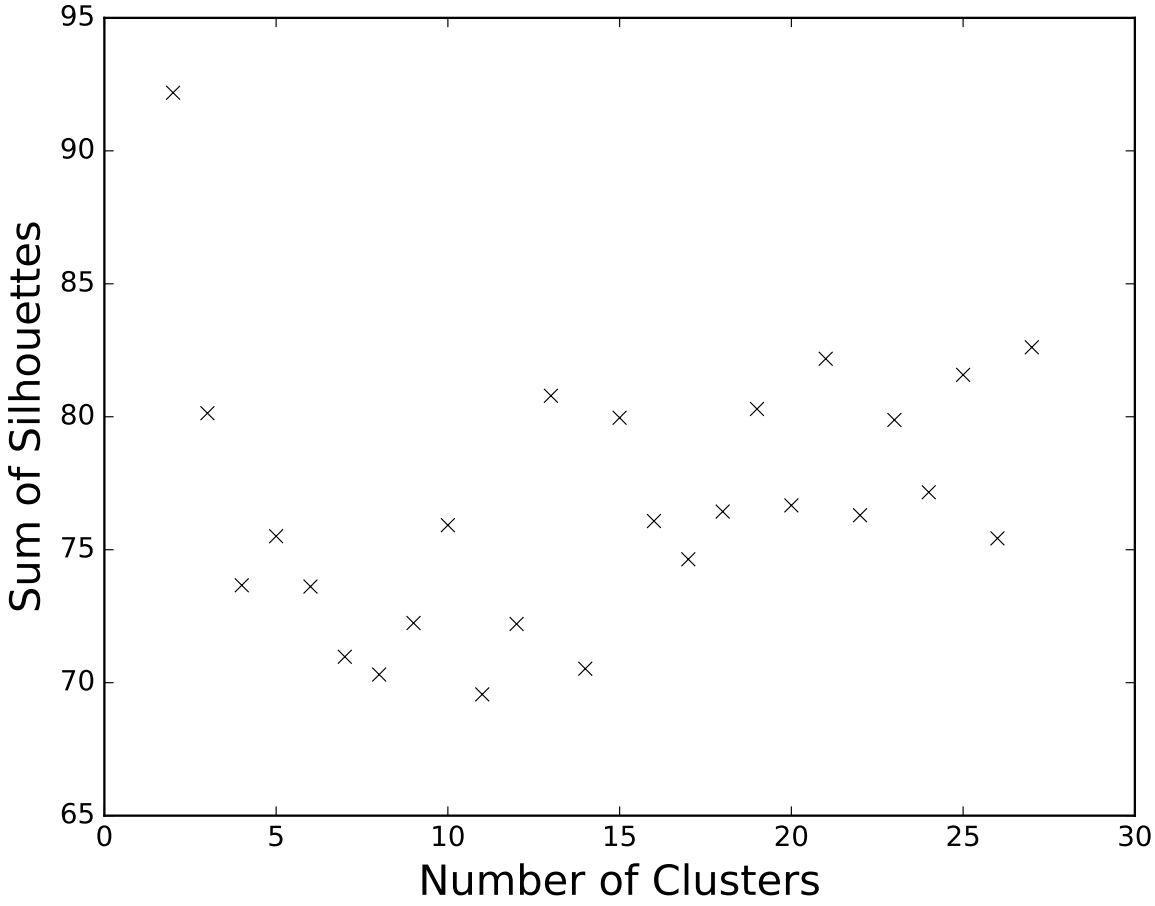

Figure 5. Sum of silhouettes as function of number of clusters

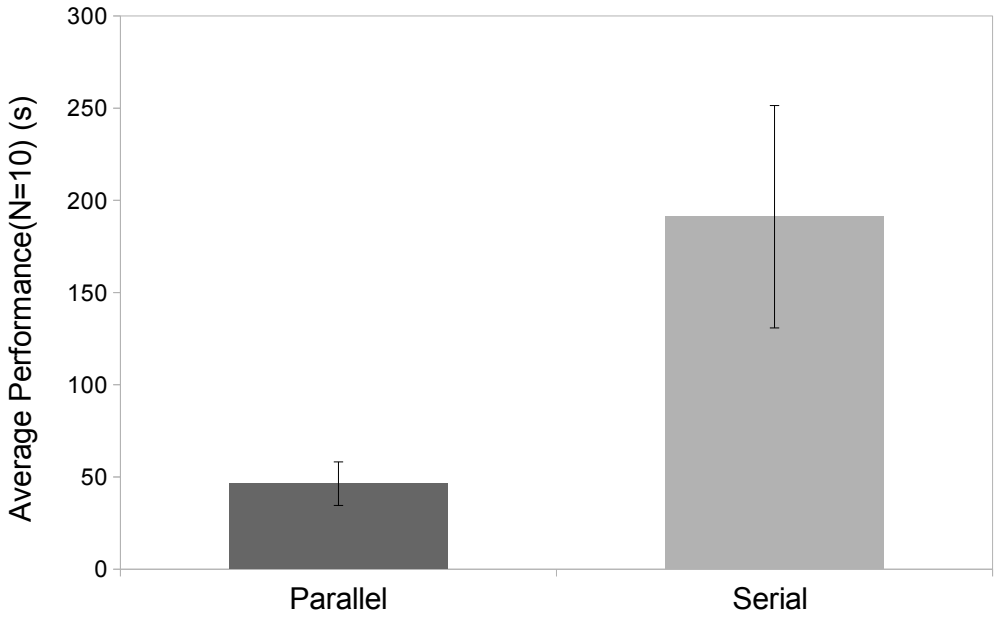

Figure 6. Switching from serial to parallel computation resulted in a significant speed up. In parallel operation, six cores were used.

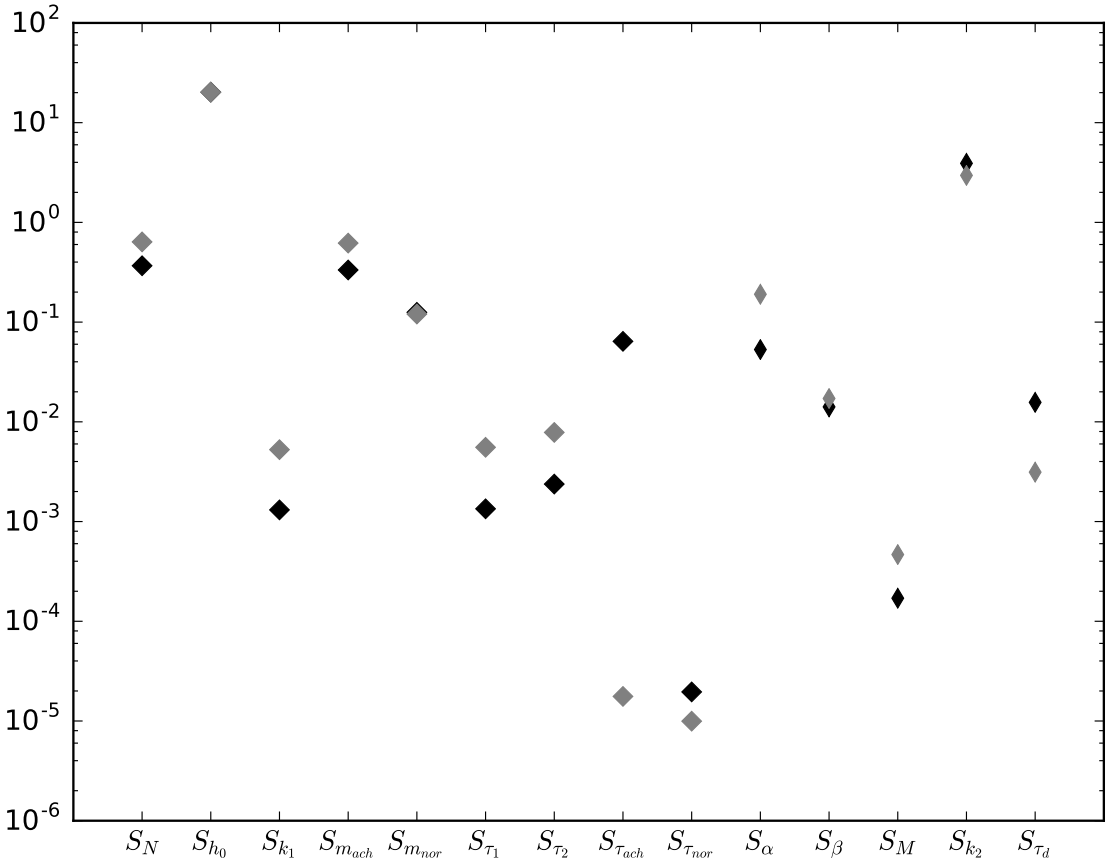

Figure 7. The black marks are from cluster 1, the grey marks represent cluster 2. Error bars are omitted for the sake of clarity. Parameters represented by an square were allowed to vary, and parameters represented by a diamond were held constant.

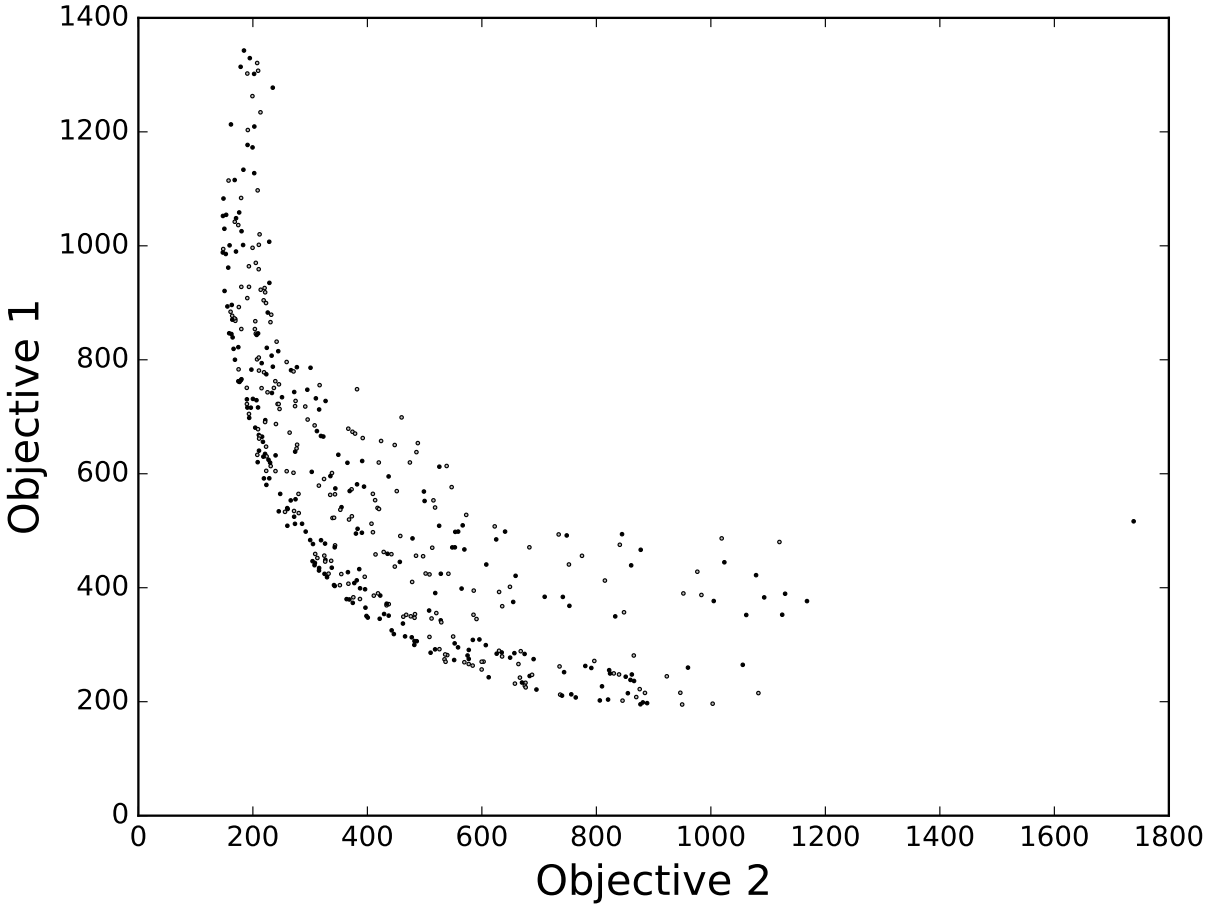

Figure 8. The black dots represent the rank 0, or best parameter sets, and the grey dots represent rank 1-4 parameter sets.

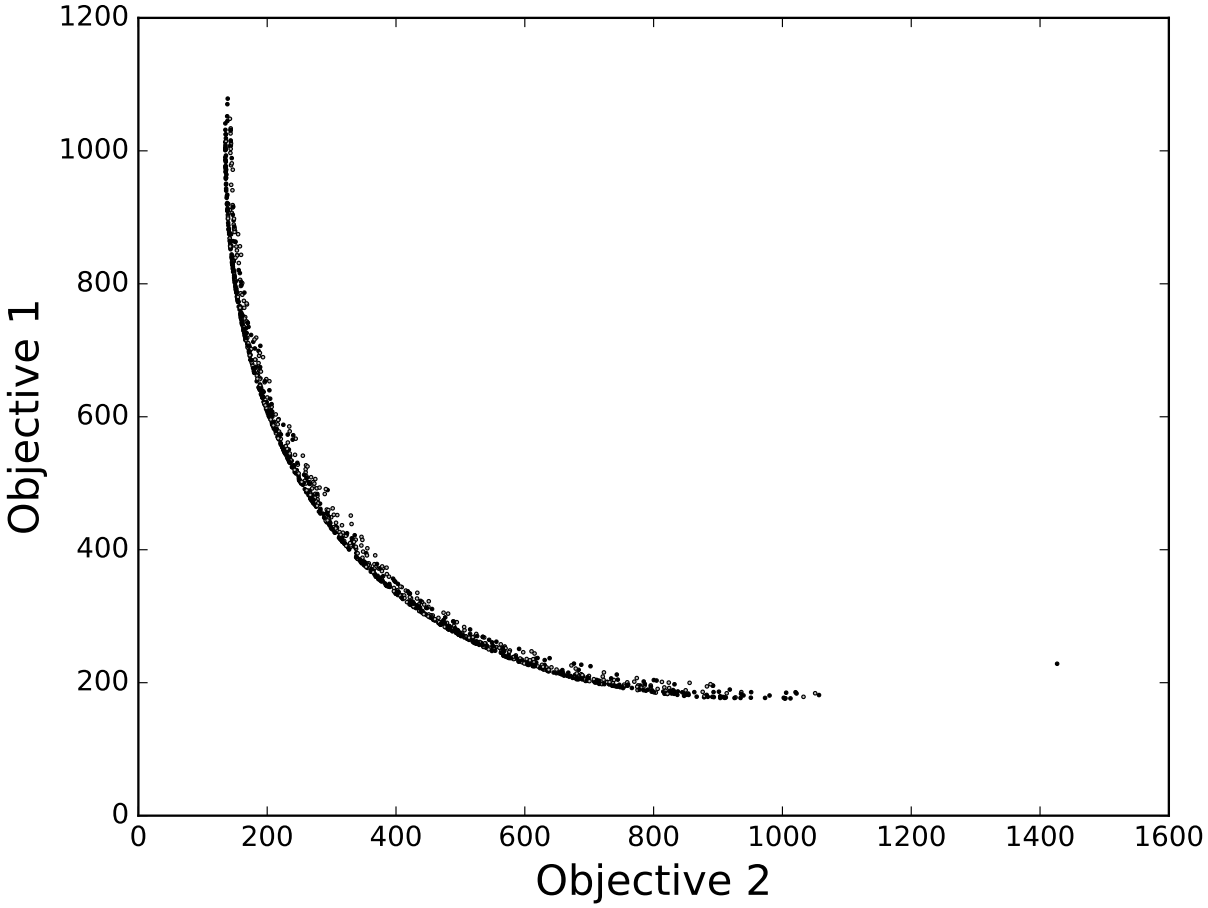

Figure 9. The black dots represent the rank 0, or best parameter sets, and the grey dots represent rank 1-4 parameter sets.